Indonesian Journal of Chemistry and Environment
Vol. 7, No. 1, June 2024, pp. 31~41
e-ISSN: 2599-3186

A novel triazole as a rapidly acetate anion detector: Synthesis, spectrophotometric, and TD-DFT studies

Sajjad Qasim Makki[1], Asim Balakit[2]
[1]Al-Shatrah University / College of the Education for Women, Iraq
[2]College of Pharmacy, University of Babylon, Iraq

Article Info
Article history:
Received Apr 1st, 2024
Revised Jun 10th, 2024
Accepted Jun 30th, 2024

Corresponding Author:
Sajjad Qasim Makki,
Al-Shatrah University / College of the Education for Women
Email: sajjad.makki@shu.edu.iq

ABSTRACT
A well- Sodium acetate has been used as a food flavor enhancer in the production of cheese, snack food, and pastry products. Hence, accurate quantification of sodium acetate content in food has significant importance within the realm of food chemistry. A Schiff-base reaction was used to produce the sensor 1,2,4 triazole derivative 3. The assessment of sensor **3**'s response to sodium salts (HSO_4-, H_2PO_4-, NO_2-, F-, Br-, Cl-, and AcO-) was conducted through naked-eye detection and subsequently confirmed using UV-vis spectroscopy. The addition of ions to sensor 3 resulted in a spectral change. Notably, only AcO- presented a unique shift in the visible spectra, while no changes were observed for the other anions. Sensor **3** has a notable level of sensitivity, as seen by the naked eye, in detecting acetate anion. The frequent addition of AcO- to a solution of sensor **3** results in an interesting color shift from light yellow to red-orange. The stoichiometry and association constant (Ka) were determined using the Benesi-Hildebrand equation, yielding values of 1:2 and $9.93x10^9$ M^{-2}, respectively. The calculation of the limit of detection (LoD) yielded a result of 6.86 μM. The synthesis of sensor **3** was confirmed using 1HNMR, IR, and UV techniques. The DT-DFT, HOMO, and LUMO values were computed using the Gaussian 09 software

Keyword: Colorimetric Sensor, Sodium acetate TD-DFT, HOMO and LUMO, 1,2,4 triazole

1. INTRODUCTION

Supermolecular chemistry has garnered significant interest in the field of anion sensing, particularly in relation to synthetic colorimetric sensors. This is primarily owing to their crucial function in many chemical, biological, environmental, and industrial applications (Qu et al., 2017; Mahanta et al., 2017; Mansha et al., 2017; Niu et al., 2018). Researchers have shown significant interest in the design and synthesis of active receptors capable of detecting anions (Zou et al., 2019; Koc et al., 2017; Li et al., 2019; Haider et al., 2020; Zhou et al., 2019; Wang et al., 2020; Tummachote et al., 2019; Nassar et al., 2017; Pinhal et al., 2019). Acetate is considered one of the most significant anionic species, because of its various biochemical functions. For example, acetate anion plays an essential role in numerous metabolic processes, having unique effects on enzyme activity, hormone transport, protein synthesis, and DNA regulation. Sodium acetate excellently inhibits bacterial growth in acidic environments according to Zhang et al. (2020), Liu et al. (2019), and Ladell et al. (2018), acetate anon has the capability to function as a buffer. colorimetric sensors are usually made up of two components: the guest (binding site) and the signaling unit. The hydrogen-bond-donor groups, specifically the -NH and OH groups of phenols (Wu et al., 2020), ureas (Cui et al., 2020), amides

(Gupta et al., 2020), and hydrazides (Xu et al., 2021), are frequently found as binding sites. Compounds containing derivatives of 1,2,4-triazole display an extensive range of applicable properties within various fields, including anticancer, antibacterial, antimicrobial, antifungal, anticonvulsant, antitumor activity, and other industrial applications (Grytsai et al., 2020; Stingaci et al., 2020; Pagniez et al., 2020; Drabik et al., 2020; Wu et al., 2020; Naciri et al., 2020). According to Mondal et al. (2020), heterocycles containing mercapto and amino groups have been found to be effective intermediates in organic synthesis. According to the pupleshed results indicates that these compounds exhibit selective chromogenic properties for Cu^{2+} ions due to the presence of (azomethine) linkages and hetero atoms as part of these compounds. Newly, scientists are concerned on the development of novel triazole Schiff bases using different azo dyes (Singh et al., 2020; Chatterjee et al., 2020). In this study, we present a novel acetate anion sensor with high sensitivity and selectivity. The sensor is designed specifically for the detection of acetate in food additives, based on Azo-triazole (Figure 01). Sensor 3 displayed a highly significant change in color in the DMSO medium.

2. RESEARCH METHOD

a. General

All commercially purchased reagents for synthesis were used without further purification. All solutions containing anions were produced using their respective sodium salts. The FT-IR, Tensor ll, Bruker-Optics, Germany spectrophotometer was used to record infrared spectra. The Bruker Avance lll was used to record proton nuclear magnetic resonance (^{1}HNMR) at a frequency of 400 MHz. The solvent used was dimethyl sulfoxide-d_6 (DMSO-d_6), and the reference used was Tetramethylsilane (TMS). The Shimadzu UV-1800 Spectrophotometer was used to measure the UV-vis spectra. The measurement of the melting points was conducted using an SMP10 melting point model, specifically the Stuart apparatus.

b. Synthesis of 3

A solution of 1 (4 mmol) in chloroform (10 ml) and a solution of 2 (4 mmol) in methanol have been placed into a round-bottomed flask. Following this, a small quantity of H_2SO_4 was added to the mixture. After refluxing the combination for a duration of 5 hours, a yellow powder was produced and obtained using filtration. Subsequently, it was rinsed with chloroform (CCl_3) (Figure 1). The yield of compound **3** was 91% and its melting point ranged from 263 to 264 degrees Celsius.

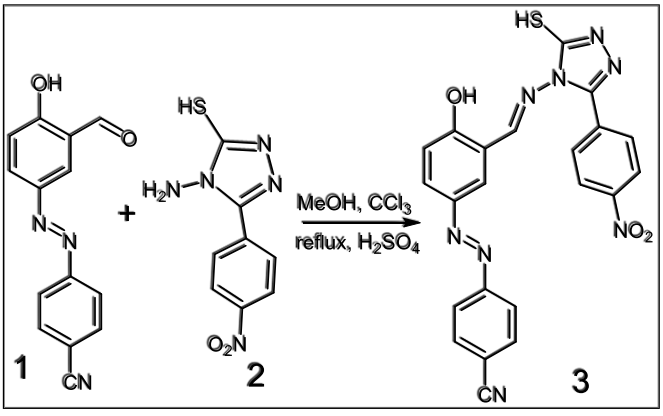

Figure 1. Synthesis of sensor **3**

c. Spectrophotometric studies

Sensor 3 stock solutions (10 μm) (100 ml) and sodium salts (HSO_4-, H_2PO_4-, NO_2-, F-, Br-, Cl, and AcO-) (50 μm) (100 ml) were individually produced in dry dimethyl sulfoxide (DMSO) and thereafter used at the surrounding temperature (30^0C).

d. (UV–vis) titration of sensor 3 with anions

A stock solution of sensor 3 (10 μM) (2 mL) was supplemented with various solutions of sodium salts (HSO_4-, H_2PO_4-, NO_2-, F-, Br-, Cl-, and AcO-) (10 μM) (2 mL). The total volume of the solution was 4 mL, and the spectra were monitored at room temperature (30°C). The Benesi-Hildebrand plot was used to estimate the association constant and stoichiometry value, as seen in Equation (1).

$$\frac{1}{\mathrm{A-Ao}} = \frac{1}{Ka \text{ x } (\mathrm{Amax-Ao}) \text{ X } [\mathrm{OAc^-}]} + \frac{1}{\mathrm{Amax-Ao}} \ldots\ldots\ldots\ldots\ldots\ldots\ldots\ldots\ldots\ldots (1)$$

A represents the measured absorbance at a certain wavelength, A_{max} indicates the highest absorbance, and *Ao* represents the lowest absorbance at a certain wavelength. *[OAc-]* represents the molar concentration, and *Ka* association constant (Li, Z. et al., 2018). The calculation of the (limits of detection) using Equation (2) according to Dong et al. (2021). The LoD is calculated as:

$$\mathrm{LoD} = \frac{3 \text{ Sy/x}}{\mathrm{S}} \ldots\ldots\ldots\ldots\ldots\ldots\ldots (2)$$

e. Computational studies

The Uv-vis spectroscopic computation was conducted using the time-dependent density functional theory (TD-DFT) approach, using functional (B3LYP) and the 6-311G++(d,p) method according to Gökalp et al. (2020). The estimation of transition energies (HOMO) and (LUMO) distribution analysis for the molecular geometry of sensor **3** was conducted using the (B3LYP)6-311G++(d,p) approach. The computations were run up using softwares Gaussian 09W (Frisch et al., 2009), GaussView6 (Dennington et al., 2009), and gaussSum3 (Salassa et al., 2009).

3. RESULTS AND ANALYSIS

Sensor **3** was synthesized by reaction of 4-[(3-Formyl-4-hydroxyphenyl)diazenyl]-benzo-nitrile) with (4-amino-5-phenyl-4H-1,2,4-triazole-3-thiol) in acidic conditions (Figure 01) resulting a yellow powder, yield 91 %. ^{1}H NMR (400 MHz, DMSO-d_6) δ 14.41 (s, 1H), 11.77 (s, 1H), 10.41 (s, 1H), 8.27 (d, J = 2.6 Hz, 1H), 8.18 – 8.08 (m, 4H), 8.06 – 8.00 (m, 3H), 7.56 (d, J = 8.7 Hz, 1H), 7.26 (d, J = 8.9 Hz, 1H), 6.69 (d, J = 2.0 Hz, 1H). FT-IR (KBr, cm^{-1}): ν 3316 (OH), 2218 (C≡N), 1600 (C=C), 1640 (C=N), 1479,1344 (NO_2).

a. UV-vis and naked-eye techniques

(Figure 2) displays the reaction of sensor **3** to several sodium salts (HSO_4-, H_2PO_4-, NO_2-, F-, Br-, Cl-, and AcO-) when dissolved in DMSO as the solvent. The addition of ions to Sensor 3 individually results in a spectrum alteration. Notably, only AcO- exhibits a unique modification in the visible spectra, while no alterations are seen in the spectra of other anions. Moreover, the presence of the acetate anion resulted in a specific changes in color, transitioning from a pale yellow coloration to a red-orange color (Figure 33).

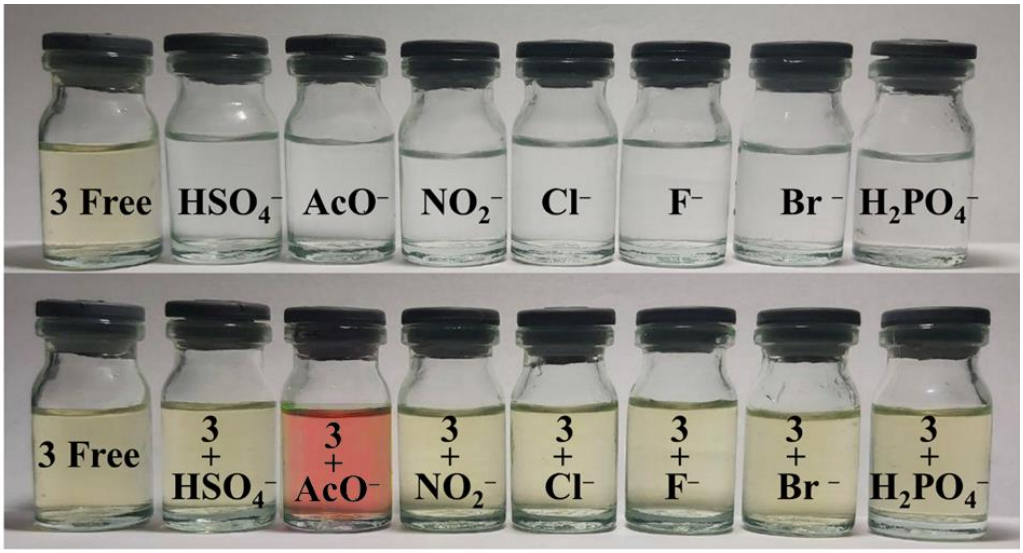

Figure 2. The colour of **3** with different anions (3 equiv.) in DMSO .

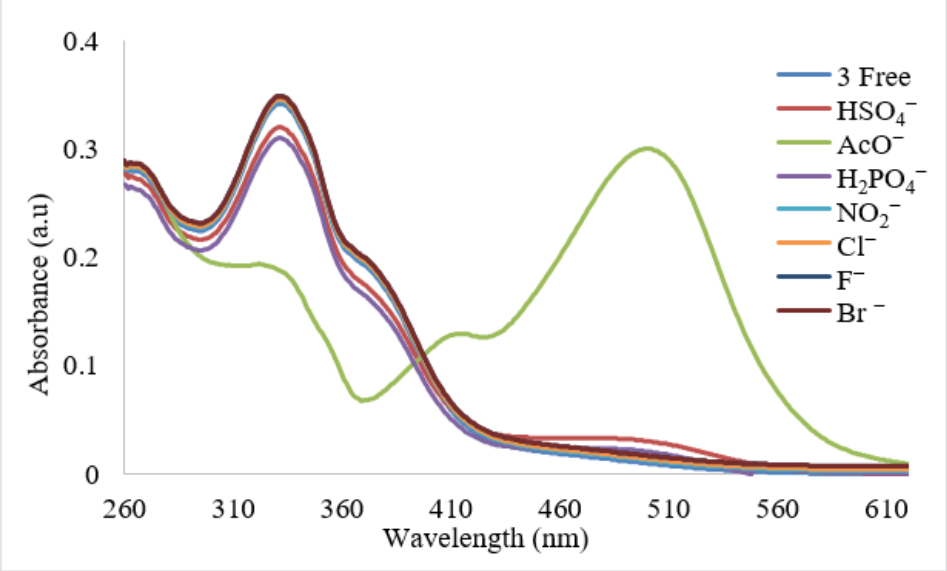

Figure 3. Changes of spectra absorption of sensor **3** with different anions in DMSO

This realization means that sensor 3 has the potential to function as a colorimetric sensor for AcO- anion that can be seen by the naked eye. Through a process addition of AcO- into a solution containing sensor 3, there was an ongoing decline in the absorption band at 331 nm, followed by the appearance of a new band at 499 nm. A significant isosbestic point was detected at a wavelength of 397 nm. The red shift seen in sensor 3 may be attributed to the internal charge transfer (ICT) and/or the deprotonation of the proton of thiol and phenol by AcO- (Figure 4).

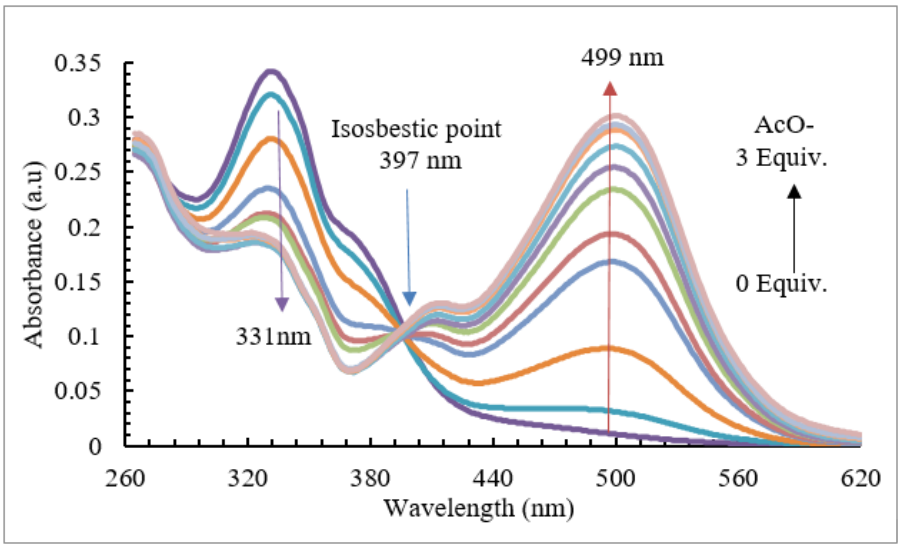

Figure 4. The titration of sensor **3** with Acetate anion (0-3 equiv.).

The Benesi-Hildebrand relation-ship was employed in order to determine the ratio or stoichiometry of the reaction between sensor 3 and AcO-. Assuming a 1:1 stoichiometry, the plot of 1/(A-Ao) against 1/[AcO-] exhibited a linear relationship with an R^2 value of 0.956 (Figure 5). In a comparable manner the plot of 1/(A-Ao) against 1/[AcO-]^2 for the 1:2 stoichiometry proved an excellent linear relationship with an R^2 value of 0.998 (Figure 66), supplying evidence that sensor **3** reacts with acetate in a 1:2 stoichiometry. The association constant (Ka) was determined to be 9.93×10^9 M^{-2} by calculation. The determination of the limit of detection (LoD) was shown in Figure 7, yielding a value of 6.86 μM.

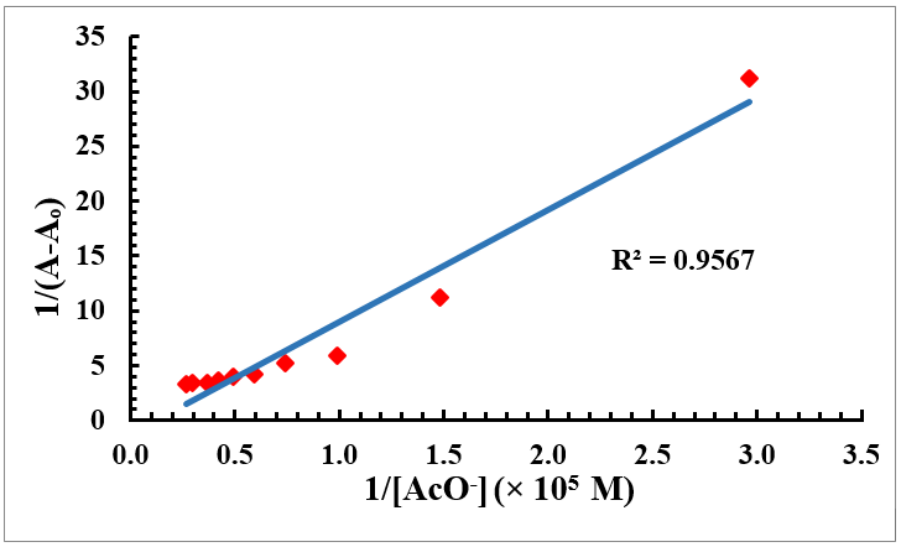

Figure 5. Benesi-Hildebrand plot of the **3** and Acetate anion (1:1 stoichiometry).

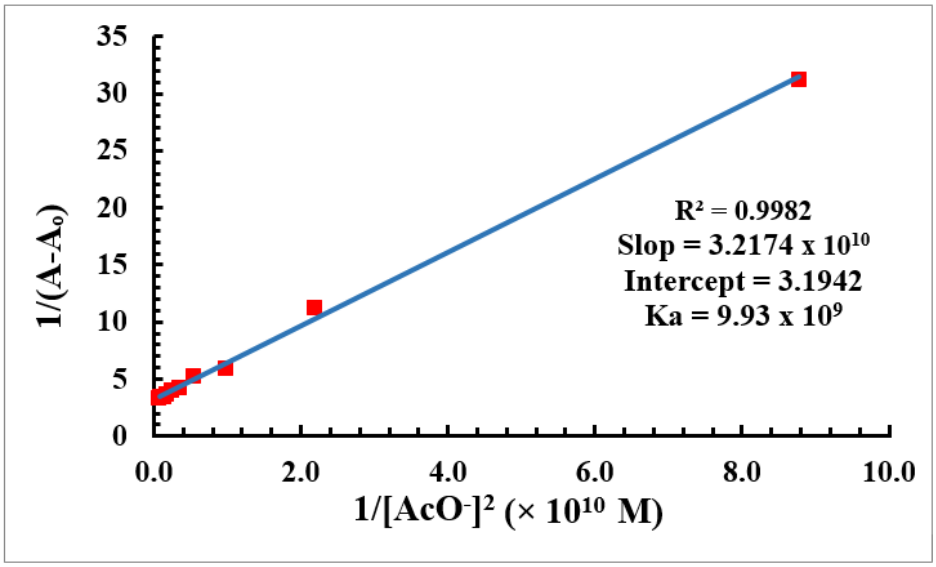

Figure 6. Benesi-Hildebrand plot of the **3** and Acetate anion (1:2 stoichiometry).

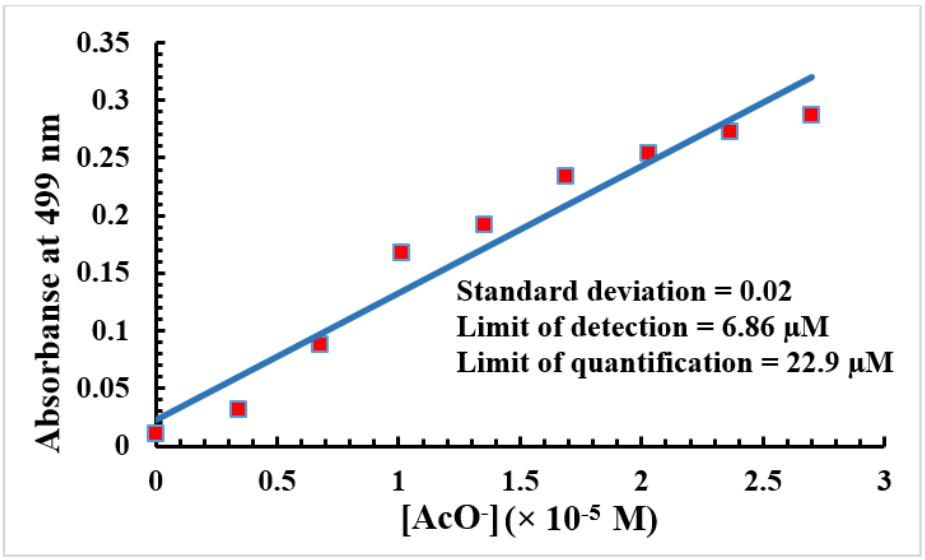

Figure 7. Limit of detection (LoD) of **3** with different concentrations of Acetate

b. Density functional theory DFT studies

The Uv-vis spectra of sensor **3** were calculated using the TD-DFT/B3LYP/6-311G++(d,p) basis set level. Theoretical calculation of UV-vis parameters has been performed using the Gaussian 09W program. The electronic transitions were analyzed using the GaussSum 3.0 program, yielding both significant and modest contributions. The energy and composition of the molecular orbitals (MOs) of **3** are briefly shown in (Table 1), as determined by calculations. The HOMO and LUMO values of sensor **3** are shown in (Figure 9). Initially, it was observed that the electron density in the highest occupied molecular orbital (HOMO) of sensor **3** is primarily concentrated on the Azo group, which is a signaling unit consisting of two aromatic rings, one of which contains a nitrile atom in the para position. On the other hand, in the lowest unoccupied molecular orbital (LUMO), the electron density is observed in the triazole group. This confirms the occurrence of intramolecular charge transfer (ICT). The addition of acetate ion resulted in an increase in absorbance intensity at 499 nm, as seen in (Figure 4). This rise was ascribed to the presence of H-2→L+1. Conversely, the absorbance at 331 nm dropped, which was related to the presence of HOMO →LUMO.(Figure 8) displays the

simulated UV-vis spectrum of **3** at wavelengths ranging from 250 to 700 nm. Display three transitions: the first transition occurs at a wavelength of 475 nm, with an oscillator strength of 0.0071 (f) and an excitation energy of 2.61 (eV). The primary contributions of the transition H-2→L+1 are 83%, while the transition H-1→L+1 makes a modest contribution of 14% for the (azo) group. The transitions occurring at wavelengths of 411 nm and 408 nm exhibit oscillator strengths of 0.0028 (f) and 0.1011 (f), respectively. The excitation energies associated with these transitions are 3.01 (eV) and 3.03 (eV). The primary contributions to these transitions are provided by the H-1→LUMO transition (98%), the HOMO →LUMO transition (91%), and the transition H-1→L+1 transition (2%).

Table 1. Electronic transitions of **3** calculated by TDDFT/B3LYP/6-311G(d,p) method .

No.	1	2	3
λ excitation (nm)	475	411	408
Excitation energy (eV)	2.61	3.01	3.03
Oscillator strength (f)	0.0071	0.0028	0.1011
Major contributions of transitions	H-2→L+1	H-1→LUMO	HOMO →LUMO
Minor contributions of transitions	H-1→L+1	--	H-1→L+1

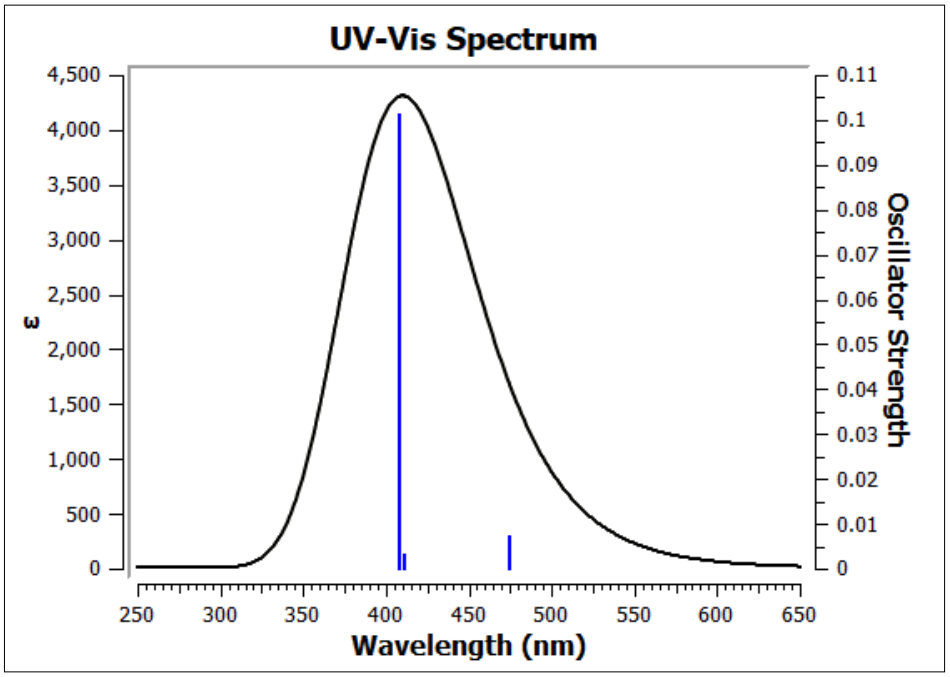

Figure 8. The virtual UV-vis spectrum at wavelength 250–700 nm of **3**

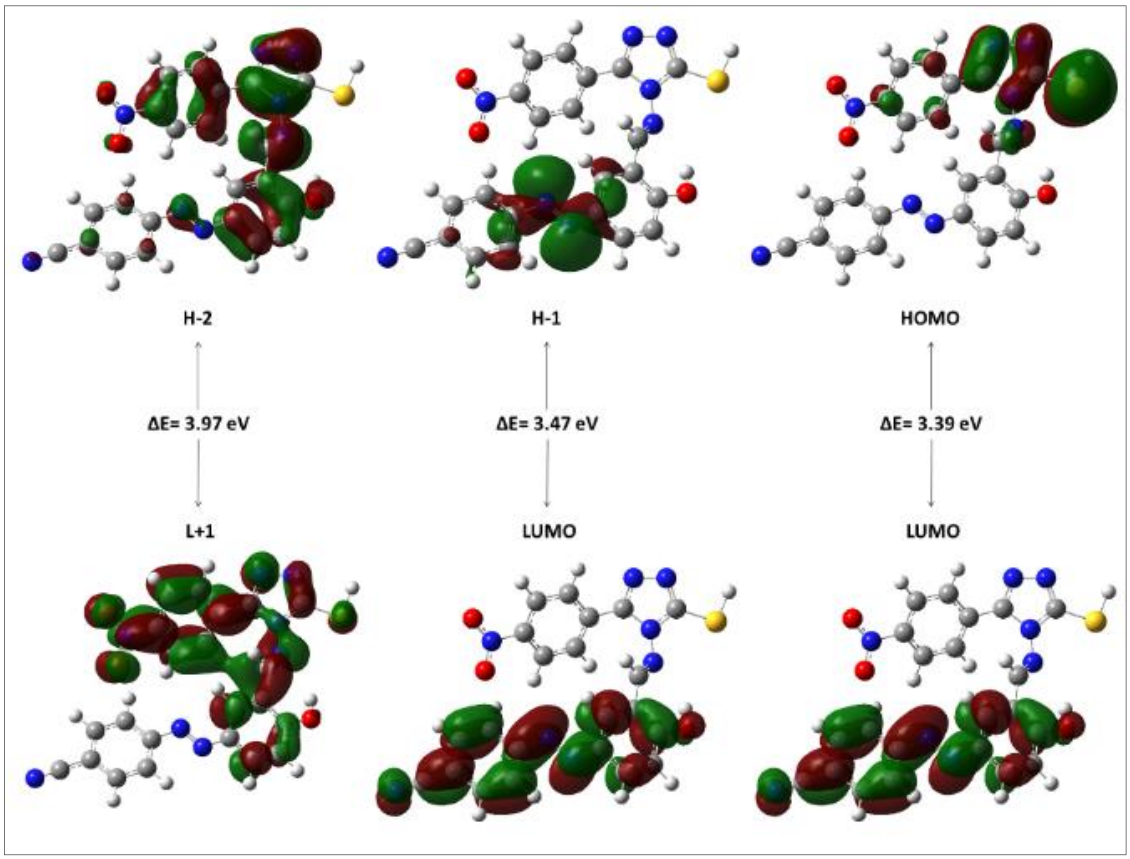

Figure 9. The HOMO and LUMO of sensor **3**

(Figure 10) suggests the proposed mechanism by which sensor 3 binds to acetate ion in DMSO solvent. This binding occurs through the deprotonation of the OH and SH groups of the sensor by the acetate anion, and/or via the formation of hydrogen bonds between the two oxygen atoms of the acetate ion and the hydrogen (OH) and (SH) within the sensor skeleton.

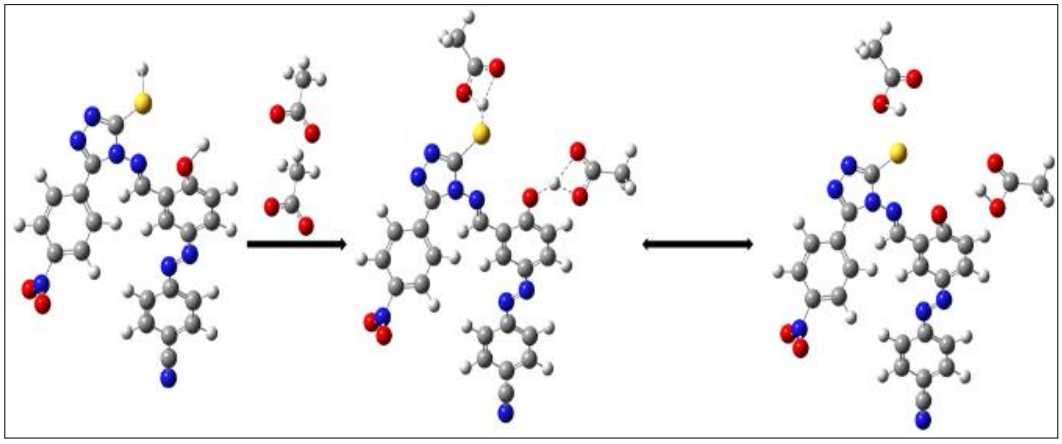

Figure 10. The suggested mechanism of the reaction between sensor **3** and Acetate anion

4. CONCLUSION

In summary, sodium acetate plays an essential part in the industry of food additives, therefore requiring the implementation of a detection technique for sodium acetate. The sensor 1,2,4 triazole derivative 3 proved to be valuable in the present study, as it exhibited an interesting color transition from light yellow to red-orange when detecting sodium acetate, allowing for easy identification without the use of microscopy. The stoichiometry and association constant (Ka) were determined to be 1:2 and 9.93 x 10^9 M^{-2}, respectively, as validated by the UV-vis spectroscopy titration tests. The determined limit of detection (LoD) was found to be 6.86 μM, indicating that 1,2,4 triazole has sensor capabilities even under conditions of low sodium acetate concentrations..

REFERENCES

Chatterjee, C., Sethi, S., Mukherjee, V., Sahu, PK, Behera, N. (2020). Triazole derived azo-azomethine dye as a new colorimetric anion chemosensor. *Spectrochimica Acta Part A: Molecular and Biomolecular Spectroscopy*, 226:117566. https://doi.org/10.1016/j.saa.2019.117566

Cui, F., Yin, G., Yang, R., Guo, X. (2020). A colorimetric chemosensor for pyrophosphate based on mono-pyrenylurea in aqueous media. *Spectrochimica Acta Part A: Molecular and Biomolecular Spectroscopy*, 241:118658. https://doi.org/10.1016/j.saa.2020.118658

Dennington, R., Keith, T., Millam, J. (2009). GaussView V. Semichem Inc. Shawnee Mission KS, *GaussView, Version:* 5

Dong, D., Yin, G., Hou, W., et al. (2021). Perylene diimide radical anion constructed by hydrogen bonds and its colorimetric chemodosimeter for the rapid detection of Fe3+. *Journal of Molecular Structure*, 1224:129038. https://doi.org/10.1016/j.molstruc.2020.129038

Drabik, M., Głuszak, M., Wróblewska-Łuczka, P., et al. (2021). Anticonvulsant Effectiveness and Neurotoxicity Profile of 4-butyl-5-[(4-chloro-2-methylphenoxy) methyl]-2, 4-dihydro-3 H-1, 2, 4-triazole-3-thione (TPL-16) in Mice. *Neurochemical Research*, 46(2):396-410. https://doi.org/10.1007/s11064-020-03175-z

Frisch, M., Trucks, G., Schlegel, H., et al. (2009). *Gaussian 09 program*. Gaussian Inc, Wallingford, CT.

Grytsai, O., Valiashko, O., Penco-Campillo, M., et al. (2020). Synthesis and biological evaluation of 3-amino-1, 2, 4-triazole derivatives as potential anticancer compounds. *Bioorganic Chemistry*, 104:104271. https://doi.org/10.1016/j.bioorg.2020.104271

Gupta, S., Mittal, SK, Chhibber, M. (2020). Triphenyl Ether Amide as a Probe for Electrochemical and Optical Sensing of Copper, Cyanide and Arginine. *Journal of the Electrochemical Society*, 167(16):167506. https://doi.org/10.1149/1945-7111/abcbb0

Gökalp, M., Dede, B., Tilki, T., Atay, ÇK. (2020). Triazole based azo molecules as potential antibacterial agents: Synthesis, characterization, DFT, ADME and molecular docking studies. *Journal of Molecular Structure*, 1212:128140. https://doi.org/10.1016/j.molstruc.2020.128140

Haider, A., Ahmed, M., Faisal, M., Naseer, MM. (2020). Isatin as a simple, highly selective and sensitive colorimetric sensor for fluoride anion. *Heterocyclic Communications*, 26(1):14-19. https://doi.org/10.1515/hc-2020-0003.

Koc, OK., Ozay, H. (2017). A simple azoquinoline based highly selective colorimetric sensor for CN− anion in aqueous media. *Canadian Journal of Chemistry*, 95(7):771-777. https://doi.org/10.1139/cjc-2017-0163

Ladell, B.A., Walleser, L.R., McCalla, S.G., Erickson, R.A., Amberg, JJ. (2019). Ethanol and sodium acetate as a preservation method to delay degradation of environmental DNA. *Conservation Genetics Resources,* 11(1):83-88. https://doi.org/10.1007/s12686-017-0955-2

Liu, L., Fu, C., Li, F. (2019). Acetate affects the process of lipid metabolism in rabbit liver, skeletal muscle and adipose tissue. *Animals*, 9(10):799. https://doi.org/10.3390/ani9100799

Li, Z., Wang, S., Xiao, L., et al. (2018). An efficient colorimetric and absorption ratiometric anion sensor based on a simple azo-azomethine receptor. *Inorganica Chimica Acta*, 479:148-153. https://doi.org/10.1016/j.ica.2018.04.027

Li, Z., Song, Y., Dai, Y., Pei, Y., Lu, Z., Guo, H. (2019). Dicyanovinyl-substituted DA type dithienylethenes: Synthesis, photochromism and colorimetric sensing for cyanide anion. *Optical Materials*, 95:109235. https://doi.org/10.1016/j.optmat.2019.109235

Mahanta, SP, Panda, PK. (2017). Bis (pyrrole-benzimidazole) conjugates as novel colorimetric sensor for anions. *Journal of Chemical Sciences*, 129(5):647-656. https://doi.org/10.1007/s12039-017-1272-8

Mansha, M., Sohail, M., Ullah, N. (2017). Synthesis, characterization, and properties of new 3-hexyl-2, 5-diphenylthiophene: Phenylene vinylenes copolymers as colorimetric sensor for iodide anion. *Journal of Applied Polymer Science*, 134(24). https://doi.org/10.1002/app.44948

Mondal, S., Kumari, C., Hira, SK, Dey, S. (2020). Dual core clickate fluorophores for selective recognition of Cu2+ and Ni2+ along with live cell imaging. *Inorganica Chimica Acta*, 509:119655. https://doi.org/10.1016/j.ica.2020.119655

Naciri, M., El Aoufir, Y., Lgaz, H., et al. (2020). Exploring the potential of a new 1, 2, 4-triazole derivative for corrosion protection of carbon steel in HCl: A computational and experimental evaluation. *Colloids and Surfaces A: Physicochemical and Engineering Aspects*, 597:124604. https://doi.org/10.1016/j.colsurfa.2020.124604

Nassar, MY, Aly, HM, Abdelrahman, EA, Moustafa, ME. (2017). Synthesis, characterization, and biological activity of some novel Schiff bases and their Co (II) and Ni (II) complexes: a new route for Co_3O_4 and NiO nanoparticles for photocatalytic degradation of methylene blue dye. *Journal of Molecular Structure*, 1143:462-471. https://doi.org/10.1016/j.molstruc.2017.04.118

Niu, Q., Lan, L., Li, T., et al. (2018). A highly selective turn-on fluorescent and naked-eye colorimetric sensor for cyanide detection in food samples and its application in imaging of living cells. *Sensors and Actuators B: Chemical*, 276:13-22. https://doi.org/10.1016/j.snb.2018.08.066

Pagniez, F., Lebouvier, N., Na, YM, et al. (2020). Biological exploration of a novel 1, 2, 4-triazole-indole hybrid molecule as antifungal agent. *Journal of enzyme inhibition and medicinal chemistry*, 35(1):398-403. https://doi.org/10.1080/14756366.2019.1705292

Pinhal S, Ropers D, Geiselmann J, de Jong H. Acetate metabolism and the inhibition of bacterial growth by acetate. Journal of bacteriology. 2019;201(13):e00147-19. https://doi.org/10.1128/jb.00147-19

Qu, W-J, Li, W-T, Zhang H-L, et al. (2017). A rational designed fluorescent and colorimetric dual-channel sensor for cyanide anion based on the PET effect in aqueous medium. *Sensors and Actuators B: Chemical*, 241:430-437. https://doi.org/10.1016/j.snb.2016.10.100

Salassa, L., Garino, C., Salassa, G., et al. (2009). Ligand-selective photodissociation from [Ru (bpy)(4AP) 4] 2+: a spectroscopic and computational study. *Inorganic chemistry*: 48(4):1469-1481 https://doi.org/10.1021/ic8015436

Singh, G., Satija, P., Singh, A., Soni, S. (2020). Azo dye featuring triazole appended organosilicon multifunctionalized sensor: Paradigm for detection of Cu+2 and Fe+2 ions. *Materials Chemistry and Physics*, 249:123005. https://doi.org/10.1016/j.matchemphys.2020.123005

Stingaci, E., Zveaghinteva, M., Pogrebnoi, S, et al. (2020). New vinyl-1, 2, 4-triazole derivatives as antimicrobial agents: Synthesis, biological evaluation and molecular docking studies. *Bioorganic & Medicinal Chemistry Letters*, 30(17):127368. https://doi.org/10.1016/j.bmcl.2020.127368

Tummachote, J., Punyain, W., Thanomsak, S., Sirikulkajorn, A., Tomapatanaget, B. (2019). Colorimetric N-butyl-3, 6-diamidecarbazole-based chemosensors for detection of fluoride and cyanide anions. *Spectrochimica Acta Part A: Molecular and Biomolecular Spectroscopy*, 214:384-392. https://doi.org/10.1016/j.saa.2019.02.081

Wang, L., Ding, H., Ran, X., Tang, H, Cao, D. (2020). Recent progress on reaction-based BODIPY probes for anion detection. *Dyes and Pigments*, 172:107857. doi: 10.1016/j.dyepig.2019.107857.